Differences between direct current and alternating current capacitance nonlinearities in high-k dielectrics and their relation to hopping conduction

O. Khaldi,[1,2] P. Gonon,[1,3,a)] C. Vallée,[1,3] C. Mannequin,[1,3] M. Kassmi,[1,2] A. Sylvestre,[4,5] and F. Jomni[2]
[1]*Univ. Grenoble Alpes, LTM, F-38000 Grenoble, France*
[2]*El Manar University, LMOP, 2092 Tunis, Tunisia*
[3]*CNRS, LTM, F-38000 Grenoble, France*
[4]*Univ. Grenoble Alpes, G2ELAB, F-38000 Grenoble, France*
[5]*CNRS, G2ELAB, F-38000 Grenoble, France*

(Received 17 July 2014; accepted 9 August 2014; published online 27 August 2014)

Capacitance nonlinearities were studied in atomic layer deposited HfO_2 films using two types of signals: a pure ac voltage of large magnitude (ac nonlinearities) and a small ac voltage superimposed to a large dc voltage (dc nonlinearities). In theory, ac and dc nonlinearities should be of the same order of magnitude. However, in practice, ac nonlinearities are found to be an order of magnitude higher than dc nonlinearities. Besides capacitance nonlinearities, hopping conduction is studied using low-frequency impedance measurements and is discussed through the correlated barrier hopping model. The link between hopping and nonlinearity is established. The ac nonlinearities are ascribed to the polarization of isolated defect pairs, while dc nonlinearities are attributed to electrode polarization which originates from defect percolation paths. Both the ac and dc capacitance nonlinearities display an exponential variation with voltage, which results from field-induced lowering of the hopping barrier energy. © *2014 AIP Publishing LLC*.
[http://dx.doi.org/10.1063/1.4893583]

I. INTRODUCTION

Metal-Insulator-Metal (MIM) capacitors are used in the microelectronic industry for mixed-signal and radio-frequency (RF) applications. For such applications, it is important to have a high level of linearity over a broad voltage range (low voltage coefficients). Regarding the voltage dependence of the capacitance, it is common to describe the capacitance-voltage (C-V) characteristic by a second-order polynomial law,

$$\frac{\Delta C}{C_0} = \alpha V^2 + \beta V, \tag{1}$$

where C_0 is the capacitance at zero bias, $\Delta C = C(V) - C_0$ is the capacitance increase at bias V, and α and β are voltage coefficients. The quadratic voltage coefficient (α) can reach up to several 1000 ppm/V^2 when materials are not optimized. It can be positive (in most high-k materials such as transition metal oxides) or negative (in silicon nitrides, silicon oxides, or in crystalline perovskites). The linear voltage coefficient (β), up to several 100 ppm/V, is introduced to take into account departure from a pure quadratic dependence (electrode effects). Usually, the quadratic term (αV^2) dominates over the linear term (βV). The origin of capacitance variation with bias (Eq. (1)) is not yet clear, and several models have been proposed.[1–8] They can be categorized as bulk vs. interface models. Bulk models refer to field-dependent ionic,[3] electronic,[6] or dipolar[8] polarizabilities, but also to electrostriction[6] or to more general thermodynamic arguments.[5] Interface models refer to interface traps[1] or to electrode polarization.[4] At present, there is not a unique model which is able to explain all the experiments. For instance, some interface models, such as the electrode polarization model,[4] are unable to explain negative α coefficients as observed in some dielectrics.[8] On the other hand, bulk phenomena cannot explain the presence of the linear term (βV). Indeed, bulk-related nonlinearities should be same whatever the sign of the electric field, i.e., $\Delta C(V)$ must be an even (symmetric) function of V and the linear term (βV) must vanish. When $\Delta C(V)$ is not symmetric,[2] the linear term must be introduced to take into account electrode/oxide interface effects, which depend on bias polarity ($V < 0$ or $V > 0$). Therefore, in the same material, different effects can coexist. An example was reported for SiO_2 where, depending on film thickness, α is negative (thick films, bulk effects were proposed by authors) or positive (thin films, interface effects were proposed).[7]

When measuring nonlinearity, i.e., C-V characteristics, it is usually assumed that V is a dc bias. The capacitor is subjected to a small ac amplitude superimposed to a large dc bias, and the dc bias is responsible for nonlinearity (this will be termed "dc nonlinearity" in the following). However, in some applications, the capacitor may be subjected to a large ac signal (with no dc bias). The question arises of what could be the magnitude of nonlinearity under large ac voltages (termed "ac nonlinearity"). In theory, a given polarization mechanism should lead to similar ac and dc nonlinearities (this will be reminded here). In practice, it will be shown that dc and ac nonlinearities could be very different. The case will be evidenced for HfO_2 thin films where ac nonlinearities are much higher than dc ones. The origin of such a difference will be related to bulk vs. interface polarization

a)Author to whom correspondence should be addressed. Electronic mail: Patrice.gonon@cea.fr.

phenomena, both being linked to hopping charge transport. The present study follows our preceding works on the electrical properties of HfO_2 in view of its application to MIM devices.[9–11]

II. EXPERIMENTS: DC VERSUS AC NONLINEARITIES

The tested MIM capacitors consist in Au/HfO_2 (10 nm)/TiN structures. HfO_2 is deposited by Atomic Layer Deposition (ALD) from $HfCl_4$ and H_2O precursors. Films are grown on TiN/Si substrates (bottom electrode), followed by the evaporation of a top gold electrode (1.5 mm in diameter). HfO_2 deposition is carried out at 350 °C, resulting in polycrystalline films (mainly orthorhombic). High resolution transmission electron microscopy (HRTEM) shows grains with random orientation, having a lateral size in the 15–20 nm range, and extending from the bottom TiN to the top Au (see HRTEM images of similar samples in Ref. 9).

Capacitance measurements are carried out using two kinds of test signals. The first (usual) one consists in a small ac voltage (0.1 V_{rms}, 1 kHz) superimposed to a dc bias varying from +1.5 V to −1.5 V (dc polarity is the one applied to the TiN electrode). It is used to probe dc nonlinearity. The second test signal consists in a pure ac voltage (1 kHz) whose amplitude varies from 0.05 V_{rms} to 2 V_{rms}. It is used to probe ac nonlinearity (Fig. 1).

Fig. 2 shows the capacitance (C) for dc and ac bias. For the dc bias case (Fig. 1(a)), C varies from 18.88 nF at 0 V, to 19.11 nF at 1.5 V. Measurements are performed using a high precision impedance analyzer (Alpha model from Novocontrol Technologies). For the above capacitance range, the absolute error of the impedance analyzer is 0.1%. This corresponds to an absolute error of around 0.02 nF on the measured capacitance. Relative error is 0.01%, which means that error between two consecutive measurements are around 0.002 nF, well below the variation observed in Fig. 1(a). C-V characteristics are asymmetric, nonlinearities being higher for positive dc bias (Au as a cathode). For positive bias, it is found that $\alpha = 4840$ ppm/V^2, $\beta = -290$ ppm/V, and for negative bias $\alpha = 2150$ ppm/V^2, $\beta = 1140$ ppm/V.

Fig. 2(b) shows C for ac bias. Remarkably, when compared to dc nonlinearities, ac nonlinearities are much higher.

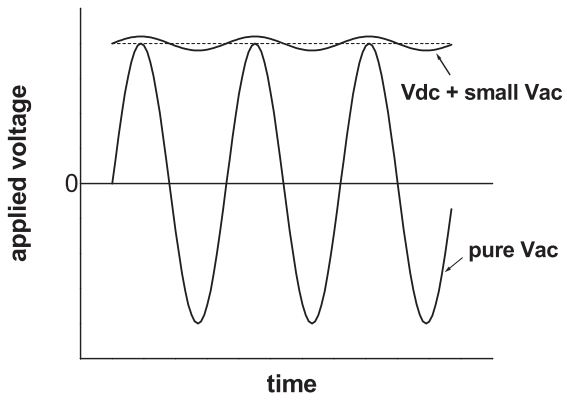

FIG. 1. Test signals used to probe dc nonlinearity (Vdc + small Vac) and ac nonlinearity (pure Vac).

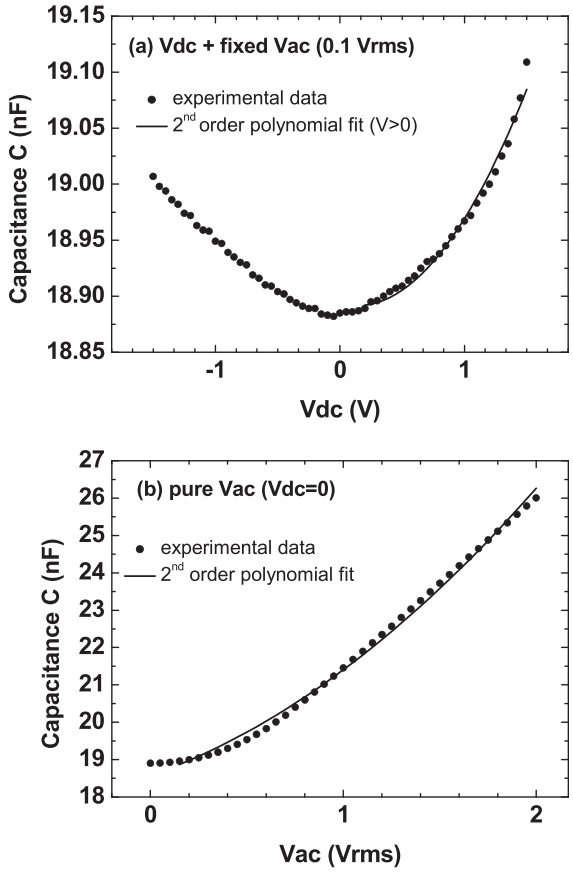

FIG. 2. Capacitance (a) vs. dc bias and (b) vs. ac bias (at 1 kHz).

For instance, for a dc bias of +1.5 V we get $\Delta C/C_0 \approx 1.2\%$, while for an ac voltage of 1.5 V_{rms} we have $\Delta C/C_0 \approx 25\%$, more than a decade above. Like dc nonlinearity, ac nonlinearity can be described by a second-order polynomial law. It is measured that $\alpha = 67\,450$ ppm/V^2, $\beta = 62\,310$ ppm/V, values which are much larger than the dc case.

To confirm the above results, measurements were repeated using a different probe station connected to a different impedancemeter (Agilent analyzer). For another sample, when the ac voltage increases from 0.1 V_{rms} to 0.7 V_{rms} (the maximum ac voltage delivered by the Agilent analyzer), capacitance increases by 11%, which is of the same order of magnitude as the C increase in Fig. 2(b). This definitely rules out any artifact which could have been related to the measurement equipment, and confirms the large magnitude of ac nonlinearity.

III. DISCUSSION

A. dc versus ac nonlinearities in theory

In theory, nonlinearities in ac and dc can be related to each other. Let us consider the electric displacement $D = \varepsilon_0 E + P$, where E is the applied electric field and P is the dielectric polarization. The electric field is composed of dc and ac parts, $E = E_{dc} + E_{ac} \sin \omega t$, then

$$D = \varepsilon_0 E_{dc} + \varepsilon_0 E_{ac} \sin \omega t + P[E_{dc} + E_{ac} \sin \omega t], \quad (2)$$

P[E] can be expressed as a power series (Maclaurin series),

$$P[E] = \sum_{0}^{\infty} \frac{P^{(n)}(0)}{n!} E^n. \quad (3)$$

Using Eqs. (2) and (3), D can be written as

$$D = \varepsilon_0 E_{dc} + \varepsilon_0 E_{ac} \sin \omega t + P_1 \times (E_{dc} + E_{ac} \sin \omega t) + P_3 \times (E_{dc} + E_{ac} \sin \omega t)^3 + \cdots, \quad (4)$$

where $P_n = P^{(n)}(0)/n!$. Since D must reverse when the polarity of E is reversed, only odd powers of E are present in Eq. (4). In the following, P_5 (and higher order nonlinearity terms) are neglected. This is justified by the fact that C(V) can reasonably be approximated by a 2nd order polynomial function (see Fig. 2). This is to say that P is approximated by a 3rd order polynomial function, and $P_n \approx 0$ as soon as $n > 3$.

Expanding $(E_{dc} + E_{ac} \sin \omega t)^3$ in Eq. (4), and considering only the terms at ω (the ones that are measured by the impedance meter), one gets the dielectric constant at ω,

$$\varepsilon(\omega) = D(\omega)/(E_{ac} \sin \omega t) = \varepsilon_0 + P_1 + (3/4)P_3 E_{ac}^2 + 3P_3 E_{dc}^2. \quad (5)$$

Note that for linear dielectrics, $P_3 = 0$, and since $P_1 = dP/dE = \varepsilon_0 \chi$, one gets the familiar expression $\varepsilon = \varepsilon_0 (1 + \chi)$, where χ is the dielectric susceptibility.

Equation (5) shows that ac nonlinearity magnitude (given by $(3/2)P_3 E_{rms}^2$, where $E_{rms} = E_{ac}/\sqrt{2}$) should be 1/2 of dc nonlinearity magnitude (given by $3P_3 E_{dc}^2$). This is derived on the basis that the same polarization mechanism governs the dc and ac response. Thus, in principle, a measure of dc nonlinearity (using a small ac signal superimposed to a dc bias) allows to predict ac nonlinearity (under a pure ac signal).

On the contrary, it is observed that ac nonlinearity is much higher than the dc one. Therefore, it is immediately apparent that P_3 in the ac term is not the same as P_3 in the dc term. In other words, two different polarization mechanisms govern the ac and dc behaviors.

B. ac nonlinearity

1. Low-frequency admittance

To get a deeper insight into physical mechanisms, the low-frequency response of the admittance ($Y = G + jC\omega$) was measured as a function of ac amplitude (Fig. 3).

At low V_{ac} (0.01, 0.1, and 0.5 V_{rms}) and at low frequency (<100 Hz), the conductance varies as ω^s, with $s = 0.8$.

$$G \sim \omega^s \ (s < 1). \quad (6)$$

This is typical of hopping conduction.[12] Exponent s increases as V_{ac} increases (>0.5 V_{rms}), to reach values close to $s = 1$ at high V_{ac}. This is shown in Fig. 4(a), where s was calculated from dG/df in the 0.1–10 Hz range, see Fig. 4(b). The increase in s with V_{ac} (Fig. 4) and the ac nonlinearity (Fig. 2(b)) appear to be correlated, as they both rise above 0.5 V_{rms}.

2. Classical theory of hopping at low ac fields

The Correlated Barrier Hopping (CBH) model[12] will be considered. Under the influence of an ac field, electrons

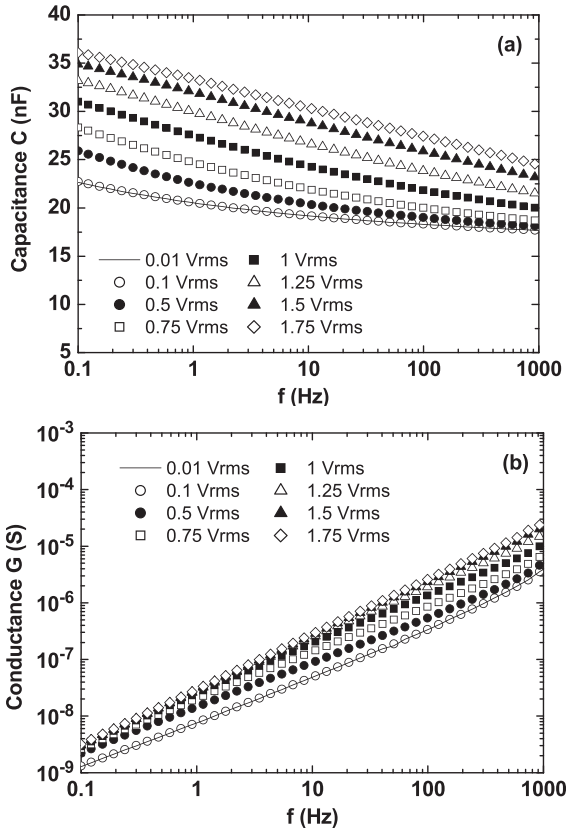

FIG. 3. Frequency dependence of (a) capacitance and (b) conductance as a function of ac amplitude (pure ac signal).

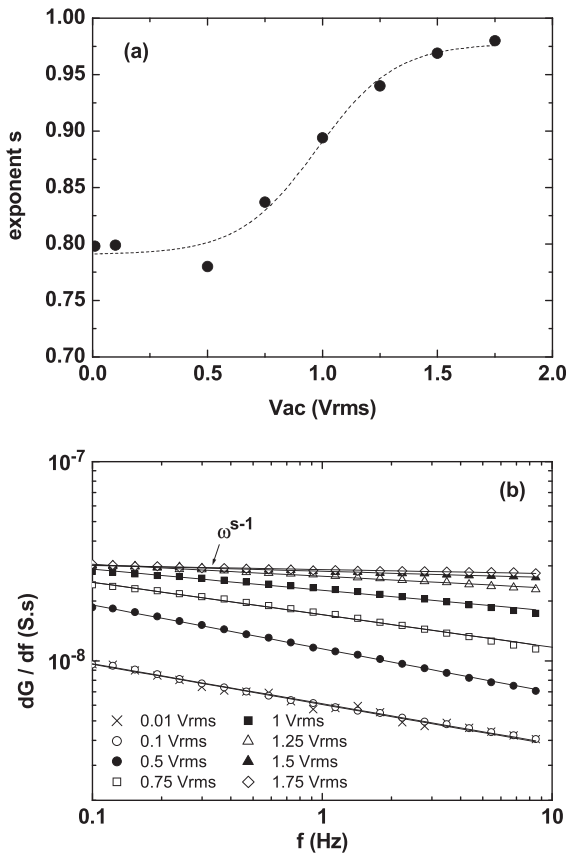

FIG. 4. (a) Hopping exponent s as a function of Vac. (b) (dG/df) vs. f, from which s was calculated.

oscillate between trap 1 and trap 2 (pair model) by hopping over a barrier W,

$$W = W_M - \frac{e^2}{\pi\varepsilon R}, \tag{7}$$

where W_M is the trap depth and R is the distance between traps. The second term in Eq. (7) is the barrier lowering due to traps overlapping (Fig. 5).[12]

Electrons hop back and forth between traps and their movement is equivalent to oscillating dipoles. Calculation of the ac conductivity requires to establish the polarization response to a step field ($E = E_0$ H(t), where H(t) is the Heaviside function) and then to operate a Fourier transform.[13] When a field E_0 is applied to the pair (direction $2 \rightarrow 1$) the electron transition rate from trap 1 to trap 2 ($1 \rightarrow 2$ hopping probability per unit of time) is

$$w_{12} = w_0 \exp(-W/kT)\exp(eE_0R/2kT), \tag{8}$$

while the $2 \rightarrow 1$ transition rate is

$$w_{21} = w_0 \exp(-W/kT)\exp(-eE_0R/2kT), \tag{9}$$

where w_0 is the attempt to escape frequency (phonon frequency).

The related characteristic time τ (relaxation time) of the equivalent oscillating dipole is given by[13]

$$\tau = 1/(w_{12} + w_{21}) = \tau_0 \exp(W/kT)/\cosh(eE_0R/2kT), \tag{10}$$

where $\tau_0 = 1/2w_0$.

At *low* fields, i.e., $eE_0R \ll 2kT$, $\cosh(eE_0R/2kT) \approx 1$ and $\tau \approx \tau_0 \exp(W/kT)$. From Eq. (7), one gets

$$\tau \approx \tau_0 \exp(W_M/kT)\exp(-e^2/\pi\varepsilon RkT). \tag{11}$$

A pair of traps, with a given separation distance R, lead to a simple Debye response in the frequency domain. However, the separation distance R varies from pairs to pairs, so does τ (see Eq. (11)). Thus, calculation has to be performed by integrating over the R distribution.[12,13] Assuming a random distribution of traps (density N), it is found[12] that

$$G = \frac{1}{24}\pi^3 \varepsilon N^2 R^6 \omega. \tag{12}$$

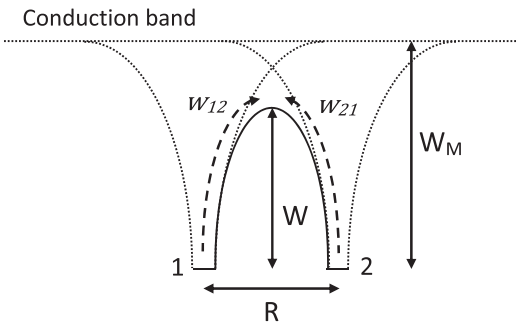

FIG. 5. Pair model (correlated barrier hopping): Trap levels 1 and 2, separated by a distance R. Trap depth is W_M, barrier between traps is W. Electron transition rate from trap 1 (2) to trap 2 (1) is w_{12} (w_{21}).

At low fields, the sub-linear dependence on frequency (Eq. (6), $s < 1$) is embedded in the R^6 term. Indeed, for a given frequency of measurement ω, major contribution to G comes from traps with a relaxation time $\tau = 1/\omega$ (resonance). However, τ depends on R (Eq. (11)). Therefore, the resonance condition $\tau = 1/\omega$ corresponds to a specific R value. From Eq. (11), one gets[12]

$$R(\omega) = (e^2/\pi\epsilon)/[W_M - kTLn(1/\omega\tau_0)]. \tag{13}$$

As ω decreases, Eq. (13) shows that the hopping distance R increases. As a consequence, the R^6 term in Eq. (12) increases as ω decreases, and this leads to the sub-linear dependence of G on ω (Eq. (6)).

3. Hopping at high ac fields

The case of high fields will now be discussed. Derivation of Eq. (12), established for low fields, is based on the Fourier transform of the step response function.[12,13] It is valid for linear systems, i.e., at low fields for which the superposition principle applies (the time response to the field $E_1 + E_2$ is the sum of the separate time responses to fields E_1 and E_2). However, at high fields the superposition principle does not apply. This is due to the field dependence of the relaxation time, Eq. (10), that leads to a Debye response for which $\tau = \tau(E)$. Therefore, the Debye response at $(E_1 + E_2)$ is not the sum of separate Debye responses at E_1 and E_2. It is no longer possible to express the polarization response to an arbitrary (high) field as the convolution of the impulse response and the field. The classical analysis (Fourier transform of the step response) leading to Eq. (12) fails. Thus, from a strict point of view, at *high* ac fields, Eq. (12) is not valid.

Calculating the frequency response of nonlinear systems from their time response is a complex mathematical task.[14] Such a calculation was not attempted here. Only a qualitative discussion will be given. As an extreme case, when $eE_0R \gg W \gg kT$ (very high fields), Eq. (10) shows that $\tau \rightarrow \tau_0$ (the minimum possible value for τ). Thus, τ is independent of R. Previously, at *low* fields, the pairs with a separation distances $R = R(\tau = 1/\omega)$ had a major contribution to ac hopping (leading to $s < 1$). Now, at very *high* fields, since τ is independent of R, all pairs equally contribute to ac hopping. This is the source of the linear variation of G with ω ($s = 1$). It is interesting to note that Eq. (12), even though it was derived at low fields, is able to predict that if R becomes independent of ω, then $G \sim \omega$ ($s = 1$).

In short, the source of ac nonlinearities is the following. As the ac field increases, more and more pairs are involved in ac hopping (not only the pairs satisfying Eq. (13)), and $s \rightarrow 1$. The increase of the number of pairs participating in ac hopping leads to an increase in bulk polarization, and C rises (Fig. 2(b)).

Up to now, a second-order polynomial law (Eq. (1)) was used to describe $C(V_{ac})$. It is a matter of usual practice and this polynomial law has no specific physical significance. It is possible to describe C(V) by an exponential law, see Fig. 6,

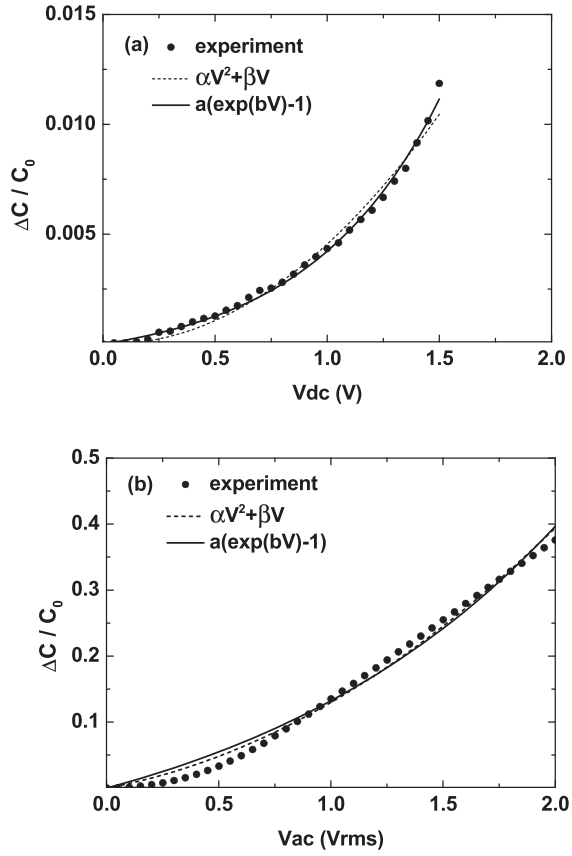

FIG. 6. Second-order polynomial law and exponential law for (a) dc nonlinearity and (b) ac nonlinearity.

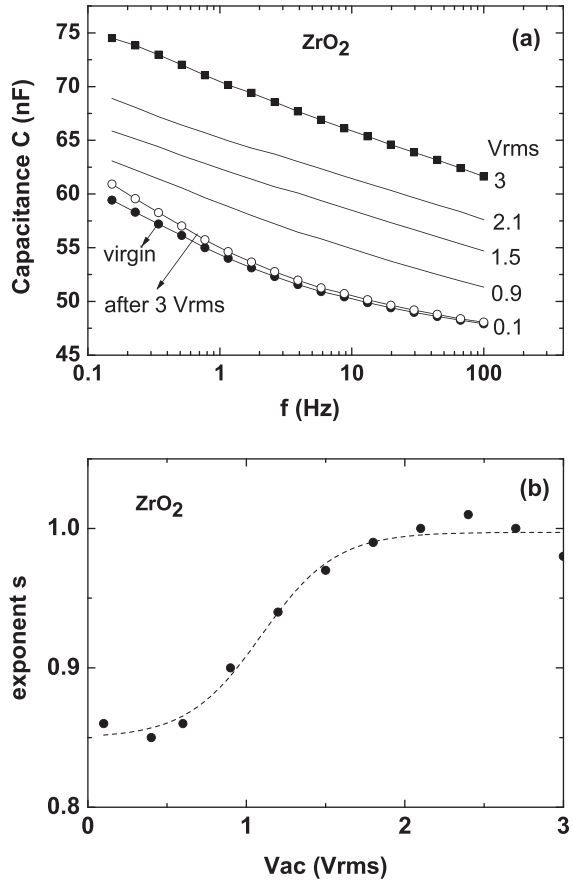

FIG. 7. (a) ac nonlinearities in ZrO_2 films and (b) s parameter extracted from the conductance.

$$\frac{\Delta C}{C_0} = a\,[\exp(bV) - 1], \tag{14}$$

where for the ac case (Fig. 6(b)), $a = 0.13$ and $b = 0.69\ V^{-1}$. The exponential law acquires physical significance because it is rooted in Eqs. (8)–(10), i.e., in barrier lowering by the field. The 2nd order polynomial law simply appears as a Taylor series expansion of the exponential law. At present, it is difficult to give analytical expressions for the parameters *a* and *b*. It would require an analytical model for ac hopping at high fields.

4. Generalization to ALD-deposited high-k oxides

To check if the above results are specific to our HfO_2 films, we also carried out measurements on ZrO_2 films which were grown in a different reactor and using different conditions (10 nm thick ZrO_2 films, deposited by Plasma-Enhanced ALD, using $(C_5H_5)Zr[N(CH_3)_2]_3$ as precursor and direct O_2 plasma as reactant).[15] As for HfO_2 films, increasing the ac voltage in the volt range leads to C increase in the 10% range (Fig. 7(a)).

Fig. 7(a) displays the capacitance at 0.1 V_{rms} after the C-f at 3 V_{rms} has been recorded. The C-f characteristic is similar to the one recorded for the virgin sample. This shows that measurements up to 3 V_{rms} (3 MV_{rms}/cm), which last several minutes, have no degradation effect on the samples. Thus, any possible oxide degradation as the source of ac nonlinearities is ruled out. In other words, ac nonlinearity is fully reversible.

As for HfO_2, ac nonlinearities in ALD-deposited ZrO_2 are linked to a change in the s exponent, which saturates to $s = 1$ at high ac voltages (Fig. 7(b)). These results tend to show that ac nonlinearities of high magnitude (a few 10%) and their relation to ac hopping are general features of ALD-grown high-k oxides.

C. dc nonlinearity

Instead of a pure ac field, we now consider the case of a large dc field to which a small ac field is superimposed. Under the influence of the large dc field, $w_{12} \gg w_{21}$ (Eqs. (8) and (9)), all carriers are stored in trap 2 and the superimposed small ac field is not able to bring back carriers to trap 1. Thus, the mechanism described in Sec. III B under pure ac field (charges oscillating between trap 1 and trap 2) vanishes.

1. Electrode polarization related to hopping conduction

Up to now, isolated and disconnected pairs were considered. However, percolation paths may exist (connected pairs). The case of conduction paths extending across the oxide thickness is now considered. Electronic charges are drifted by the dc electric field along these paths. Depending

on the efficiency of charge transfer at electrodes, space charge layers build-up at electrodes. "Blocking" electrodes correspond to bad charge transfer at the oxide/metal interface and lead to accumulation and depletion layers at the anode and at the cathode ("bad" charge transfer means that charge mobility across the interface is lower than charge mobility along hopping conduction paths). At the opposite, "Ohmic" electrodes correspond to free electronic transport across the oxide/metal interface and no space charge is present. The effect of the ac field, which is superimposed to the dc field, is to modulate the electrode space charges, giving rise to a supplementary capacitance. This is often termed "electrode polarization." It is equivalent to a macroscopic dipole whose charges are the depletion and accumulation layers and whose length is equal to the oxide thickness.

Modeling of electrode polarization was the subject of several works in the past.[16–18] In a previous publication,[4] we demonstrated that electrode polarization can account for dc nonlinearity in MIM capacitors. Briefly, we considered that the dc bias leads to a field-enhanced conductivity,

$$\sigma = \sigma_0 \exp(eE_{eff}R/2kT), \tag{15}$$

where σ_0 is the low-field dc conductivity and E_{eff} is the effective field which governs hopping along chains of defects (meaning of "effective" field is discussed below). Field-dependent conductivity, of the form given by Eq. (15), is commonly observed for electronic hopping in transition metal oxides.[19] It is a consequence of barrier lowering by the electric field, see Eq. (8).

By inserting Eq. (15) in the model of Beaumont and Jacobs[17] for electrode polarization in solids, we showed that[4]

$$\frac{\Delta C}{C_0} = \frac{2}{\varepsilon^{2n}}\left(\frac{L}{L_D}\right)^{1-2n}\frac{1}{(\rho+2)^{2(1-n)}}\frac{1}{\omega^{2n}} \times \sigma_0^{2n}\left[\exp\left(neE_{eff}R/kT\right)-1\right], \tag{16}$$

where L is the oxide thickness, L_D is the Debye length of accumulation/depletion layers, n is an empirical parameter which accounts for the variation of C with f (for hopping transport, $2n = 1 - s$, where s is the exponent appearing in Eq. (6)). Parameter ρ is the "blocking parameter" which measures charge exchange at the electrode. For "ohmic" contacts, $\rho \to \infty$, there are not any space charge layers and electrode polarization vanishes. For "blocking" contacts, $\rho \to 0$, large space charge layers exist and electrode polarization reaches a maximum value.

The exponential dependence of $\Delta C/C_0$ on V, as predicted by Eq. (16), is verified experimentally (see Fig. 6(a)). Using the general form as given by Eq. (14), we find $b = 1.7\ V^{-1}$ (and $a = 9.4 \times 10^{-4}$). If the electric field is taken as the macroscopic field, $E_{eff} = V_{dc}/L$, then $b = (neR)/(LkT)$. Since $s = 0.80$ (see Fig. 4(a), low ac fields), then $n = (1 - s)/2 = 0.10$. Then, the hopping distance is calculated to be $R = 44$ Å. Such a value is very large when compared to interatomic distances, and therefore it appears unreasonable. This problem was underlined and discussed by Austin and Sayer[19] who found hopping distances of the same order of magnitude in several transition metal oxides. According to these authors, large values of R stem from under-estimating the electric field. They postulated that the field appearing in Eq. (15) is not the Maxwell macroscopic field (V/L), but an "effective" field which results from fluctuations in energy barriers along the percolation path. Indeed, small fluctuations in local order lead to fluctuations in energy barrier. Pairs with highest energy barriers are those offering nodes with maximum resistance, i.e., nodes where the voltage drop is the highest, so does the field. Therefore, the electric field is not constant along the percolation path, being enhanced at pairs of highest energy barrier. For instance, in transition metal oxides, Austin and Sayer calculated field enhancement factors (p) varying between 4 and 17.[19] It means that the "effective" (local) field is p times higher than the average field,

$$E_{eff} \approx pxV_{dc}/L, \tag{17}$$

where p is around 10. Using $p \approx 10$, it is found $R \approx 4$ Å, which is now consistent with interatomic distances.

2. Oxygen vacancies as traps

The nature of the traps will now be discussed. For such a purpose, we refer to our previous study[11] where the activation energy of dc conductivity was measured at low fields ($V = 0.1$ V). The activation energy of the dc conduction was found to be non-constant with temperature (the slope of σ vs. 1/T is non-linear). This is consistent with a distribution of energy barriers. At room temperature, the activation energy was around 0.3 eV.[11] An activation energy around 0.3 eV was independently reported by other groups.[20,21] Since this activation energy was reported for low fields, it corresponds to R_{min} (the shortest hopping distance is the one offering the lowest barrier, see Eq. (7), i.e., the favored path for dc conduction at low fields). Oxygen vacancies are common defects in oxides. The distance between nearest-neighbored oxygen vacancies is around 3 Å in HfO_2.[22] From Eq. (7), taking $W = 0.3$ eV and $R_{min} = 3$ Å, one gets $W_M \approx 2$ eV. Such a trap depth is in agreement with levels related to oxygen vacancies (quoted around 2 eV for V_O^0 [Ref. 23], and in the 1.7 eV–2.7 eV range for V_O^+ [Ref. 24]). Therefore, oxygen vacancies could be the traps that are involved in hopping conduction.

3. Electrode polarization vs. isolated pair polarization

Electrode polarization must also be considered for ac nonlinearity (pure ac voltage, Sec. III B). However, it involves conduction paths extending across the oxide thickness. Such percolation paths are expected to involve a small fraction of the total amount of defect pairs. Therefore, under pure ac fields the polarization at isolated pairs dominates (mechanism described in Sec. III B). As reminded at the beginning of this section, when a large dc voltage is superimposed to the ac voltage, polarization at isolated pairs vanishes and the electrode polarization (of much smaller magnitude) emerges. This is schematized in Fig. 8.

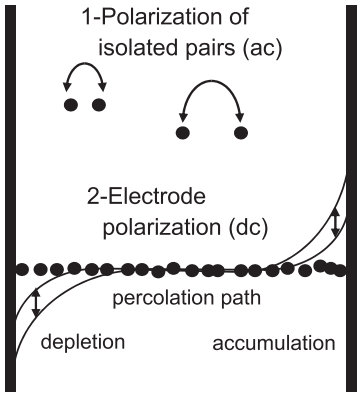

FIG. 8. Polarization which is related to isolated pairs (major contribution to ac nonlinearity) and to percolation paths (electrode polarization, the only contribution to dc nonlinearity).

IV. CONCLUSIONS

Capacitance nonlinearities, i.e., the variation of C with V, were studied in MIM structures fabricated from ALD deposited HfO_2 thin films (10 nm). Usually, nonlinearities are tested with a dc bias.[1–8] Here, we used two types of signals: a small ac voltage superimposed to a large dc bias (this is the usual configuration, used for the purpose of testing "dc nonlinearities"), and a pure ac voltage of large magnitude (for the purpose of testing "ac nonlinearities"). The goal was to compare the MIM capacitor response under dc and ac conditions. This is an important reliability issue for applications for which MIM devices can be subjected to both types of signals. In theory, ac and dc nonlinearities should be of the same order of magnitude, with the ac one being $1/2$ of the dc one. This is true if ac and dc nonlinearities originate from the same polarization mechanism. In practice, ac nonlinearities are found to be an order of magnitude higher than dc nonlinearities (artefacts which would have been related to the electrical equipment have been ruled out).

Large differences between ac and dc nonlinearities point out that different polarization mechanisms coexist. In order to identify microscopic mechanisms, low-frequency impedance spectroscopy was carried out. The study was focused on the G-ω characteristics. At low ac electric fields, we got $G \sim \omega^s$, where $s = 0.8$. This is typical of hopping conduction.[12] Within the CBH model,[12] electron hopping proceeds through isolated defect pairs with a random distribution of defect separation distance (R). A given ω corresponds to a given value of R, i.e., only a fraction of the pairs participate in hopping (this is the origin of the sub-linear dependence of G on ω). When the ac field is increased in the MV/cm range, the hopping exponent (s) progressively increases to a value close to 1 ($s \approx 1$). The departure from the value $s = 0.8$ is clearly correlated with the onset of ac nonlinearities, suggesting that both phenomena have the same origin. The rise of the s parameter is thought to originate from an increase in the number of pairs which participate in ac hopping. Since each (isolated) pair behaves as a microscopic oscillating dipole, the overall bulk polarizability increases, and C rises (source of ac nonlinearities).

The source of dc nonlinearities is electrode polarization. Such a mechanism refers to the modulation of electrode space charge regions (by the small ac test signal which is superimposed to the dc bias). This process requires dc conduction paths from one electrode to the other, i.e., connected pairs that lead to percolation paths through the film thickness (grain boundaries for instance). It differs from the preceding ac polarization mechanism (CBH) which involved isolated pairs. When applying a large dc field, ac polarization at isolated pairs vanishes (because dipole orientation is "locked-on" by the dc field). As a consequence, only the electrode polarization mechanism remains and can be observed. Modelling of dc nonlinearities is carried out using theories of electrode polarization,[17] taking into account a field-dependent dc hopping conduction, which includes a local field correction.[19] The capacitance-voltage relations can be described by an exponential law (in both the dc and ac modes). This is physically related to a lowering of the hopping barrier at large electric fields. Such an exponential law has to be contrasted with a second-order polynomial law, which is often used to describe C-V characteristics.

Though different polarization mechanisms are at the origin of ac and dc nonlinearities, they are both related to electronic hopping at oxygen vacancy defects. The related trap depth is around 2 eV, which is consistent with levels reported for oxygen vacancies in HfO_2.[23,24] Large differences between ac and dc nonlinearities are also reported for ZrO_2 thin films (which have been grown in a different ALD equipment). This suggests that the behavior is general to high-k transition metal oxides, which are slightly oxygen deficient.

Finally, from the application point of view, the present study demonstrates that it is important to perform ac tests for evaluating the voltage linearity of high-k MIM capacitors. Indeed, the usual dc bias test may largely underestimate nonlinearities which originate from the ac part of the voltage. This could become a serious reliability issue for applications where harmonics of large magnitude are present.

ACKNOWLEDGMENTS

Région Rhône-Alpes is gratefully acknowledged for financial support ("CMIRA" France-Tunisia mobility program and "Micro-Nano" research program). This work was partly supported by "Laboratoire d'Excellence" MINOS (project ANR-10-LABX-55-01).

[1]J. A. Babcock, S. G. Balster, A. Pinto, C. Dirnecker, P. Steinmann, R. Jumpertz, and B. El-Kareh, IEEE Electron Device Lett. **22**, 230 (2001).
[2]S. Van Huylenbroeck, S. Decoutere, R. Venegas, S. Jenei, and G. Winderickx, IEEE Electron Device Lett. **23**, 191 (2002).
[3]S. Bécu, S. Crémer, and J.-L. Autran, Appl. Phys. Lett. **88**, 052902 (2006).
[4]P. Gonon and C. Vallée, Appl. Phys. Lett. **90**, 142906 (2007).
[5]S. Blonkowski, Appl. Phys. Lett. **91**, 172903 (2007).
[6]Ch. Wenger, G. Lupina, M. Lukosius, O. Seifarth, H.-J. Müssig, S. Pasko, and Ch. Lohe, J. Appl. Phys. **103**, 104103 (2008).
[7]S. D. Park, C. Park, D. C. Gilmer, H. K. Park, C. Y. Kang, K. Y. Lim, C. Burtham, J. Barnett, P. D. Kirsch, H. H. Tseng, R. Jammy, and G. Y. Yeom, Appl. Phys. Lett. **95**, 022905 (2009).
[8]T. H. Phung, P. Steinmann, R. Wise, Y.-C. Yeo, and C. Zhu, IEEE Electron Device Lett. **32**, 1671 (2011).
[9]C. Mannequin, P. Gonon, C. Vallée, L. Latu-Romain, A. Bsiesy, H. Grampeix, A. Salaün, and V. Jousseaume, J. Appl. Phys. **112**, 074103 (2012).

[10]C. Mannequin, P. Gonon, C. Vallée, A. Bsiesy, H. Grampeix, and V. Jousseaume, J. Appl. Phys. **110**, 104108 (2011).
[11]P. Gonon, M. Mougenot, C. Vallée, C. Jorel, V. Jousseaume, H. Grampeix, and F. El Kamel, J. Appl. Phys. **107**, 074507 (2010).
[12]For a review on ac hopping transport, see, for instance, S. R. Elliott, Adv. Phys. **36**, 135 (1987).
[13]M. Pollak and T. H. Geballe, Phys. Rev. **122**, 1742 (1961).
[14]See, for instance, H. Zhang and S. A. Billings, Mech. Syst. Signal Process. **7**, 531 (1993).
[15]A. Salaün, H. Grampeix, J. Buckley, C. Mannequin, C. Vallée, P. Gonon, S. Jeannot, C. Gaumer, M. Gros-Jean, and V. Jousseaume, Thins Solid Films **525**, 20 (2012).
[16]J. Ross Macdonald, Phys. Rev. **92**, 4 (1953).
[17]J. H. Beaumont and P. W. M. Jacobs, J. Phys. Chem. Solids **28**, 657 (1967).
[18]B. Martin and H. Kliem, J. Appl. Phys. **98**, 074102 (2005).
[19]I. G. Austin and M. Sayer, J. Phys. C: Solid State Phys. **7**, 905 (1974).
[20]G. Bersuker, J. H. Sim, C. S. Park, C. D. Young, S. V. Nadkarni, R. Choi, and B. H. Lee, IEEE Trans. Device Mater. Reliab. **7**, 138 (2007).
[21]J. H. Kim, T. J. Park, M. Cho, J. H. Jang, M. Seo, K. D. Na, C. S. Hwang, and J. Y. Won, J. Electrochem. Soc. **156**, G48 (2009).
[22]N. Capron, P. Broqvist, and A. Pasquarello, Appl. Phys. Lett. **91**, 192905 (2007).
[23]K. Xiong, J. Robertson, M. C. Gibson, and S. J. Clark, Appl. Phys. Lett. **87**, 183505 (2005).
[24]G. Bersuker, D. C. Gilmer, D. Veksler, P. Kirsch, L. Vandelli, A. Padovani, L. Larcher, K. McKenna, A. Shluger, V. Iglesias, M. Porti, and M. Nafría, J. Appl. Phys. **110**, 124518 (2011).